Article ID: 1006-8775(2015) S1-0023-11

DIFFERENT EVOLUTIONS OF THE PHILIPPINE SEA ANTICYCLONE FOR THE IMPACT OF EL NIÑO IN PEAK PHASES WITH AND WITHOUT A POSITIVE INDIAN OCEAN DIPOLE

LI Yan (李 琰)[1, 2], WANG Qing-yuan (王庆元)[3], MU Lin (牟 林)[1], LI Huan (李 欢)[1], SONG Jun (宋 军)[1], WANG Guo-song (王国松)[1], WANG Hui (王 慧)[1]

(1. National Marine Data and Information Service, Tianjin 300171 China; 2. Key Laboratory of Global Change and Marine-Atmospheric Chemistry, Xiamen 361005; 3. Tianjin Meteorological Observatory, Tianjin 300074 China)

Abstract: The different impacts of El Niño during peak phases with and without a positive Indian Ocean Dipole (P-IOD) on the Northwest Pacific circulation were studied. The authors focused on the Northwest Pacific circulation features in the mature phase of El Niño from September to February of the next year. Composite maps and simulations demonstrate that the atmospheric circulation under the impact of El Niño with and without P-IOD exhibits large differences in temporal evolution and intensity. In single El Niño (SE) years without a P-IOD, an anomalous low-level anticyclonic circulation around the Philippines (PSAC) is instigated by the single El Niño-induced Indonesian subsidence. However, during the years when El Niño and a P-IOD matured simultaneously, a much greater anomalous subsidence over the western Pacific and the Maritime Continent occurred. The PSAC tends to occur earlier, is much stronger and has a longer lifetime than that during SE. More importantly, the PSAC shows a characteristic of an eastward movement from the southern South China Sea (SCS) to the Philippine Sea. This characteristic does not appear during SE. These patterns imply that a positive IOD event tends to exert a prominent influence on the PSAC during El Niño events and there is a combined impact of El Niño and P-IOD on the development of the PSAC.

Key words: El Niño; Indian Ocean Dipole (IOD); precipitation; atmospheric circulation; simulation
CLC number: P456 **Document code:** A
doi: 10.16555/j.1006-8775.2015.S1.003

1 INTRODUCTION

The Northwest Pacific (NWP) is located between the central-eastern Pacific and Indian Oceans and near the Asian continent. The atmospheric circulation anomalies over the NWP play an important role in the relationship between the El Niño-Southern Oscillation (ENSO) and the western North Pacific-East Asian climate systems (Yan et al.[1]; Chung et al.[2]; Chou[3]; Wang et al.[4]; Wang et al.[5]). Wang et al.[5] found that the key system linking the tropical Pacific warming and the East Asian climate was the anomalous low-level anticyclone dominating over the Philippine Sea, known as the Philippine Sea anticyclone (PSAC). In the case of El Niño, the PSAC often persists from the boreal autumn to next early boreal summer and induces a weak NWP summer monsoon in the ENSO decaying year. This lingering PSAC can bring wet conditions to southern China and tends to induce positive rainfall anomalies in the region (Wu et al.[6]; He et al.[7]; Li et al.[8]).

Another well-known coupled ocean-atmosphere phenomenon over the tropical Indian Ocean (TIO), known as the Indian Ocean Dipole (IOD), has been extensively studied in recent years (Saji et al.[9]; Webster et al.[10]; Luo et al.[11]; Xiang et al.[12]). The IOD is characterized by an anomalous east-to-west SST gradient along the TIO. A positive IOD (P-IOD) event is considered to be associated with a warmer water area in the western tropical Indian Ocean (WTIO) and a colder water area in the southeastern tropical Indian Ocean (SETIO), whereas a negative IOD (N-IOD) creates the opposite distribution of the SSTAs. IOD events usually begin to develop in boreal summer, peak in boreal fall, and decay rapidly in

Received 2014-05-14; **Revised** 2015-09-02; **Accepted** 2015-09-15
Foundation item: Program of National Natural Science Foundation of China (41106004, 41206013, 41376014); National Marine Public Welfare Research Project of China (201005019); Project of the Ministry of Science and Technology of China (2014BAB12B02); Project of the Ministry of Science and Technology of Tianjin (14ZCZDSF00012); Fund of Key Laboratory of Global Change and Marine-Atmospheric Chemistry, SOA (GCMAC 1402)
Biography: LI Yan, Ph. D., senior engineer, primarily undertaking research on climate and climate change.
Corresponding author: MU Lin, e-mail: moulin1977@hotmail.com

boreal winter[9, 12].

Approximately 45% of IOD events co-occur with ENSO; for example, P-IOD events co-occurred with El Niño in 1982 and 1997 and N-IOD events co-occurred with La Niña in 1971 and 2005 (Meyer et al.[13]; Saji and Yamagata[14]). However, several El Niño events have occurred without P-IOD or occurred with N-IOD. Consequently, these two types of events are noteworthy. In this paper, a single El Niño without P-IOD is referred to as SE and an El Niño with P-IOD is referred to as EPI. Here, an SE year is defined as a year when an El Niño matures solely during boreal winter. An EPI year is defined as a year when El Niño peaks in boreal autumn-winter and a P-IOD peaks in boreal autumn. Researchers have found that both the SE and EPI events can greatly affect the climate variability in local and remote regions (Ashok[15, 16]; Guan and Yamagata[17]; Hong et al.[18]; Cherchi and Navarra[19]). However, the different impacts of El Niño during peak phases with and without a P-IOD on the PSAC have received little attention. Two questions remain to be answered: (1) Is there any difference in the temporal evolution and the strength of the PSAC under the impacts of the SE and EPI? (2) What are the mechanisms underlying the effects of the two types of El Niño on the PSAC?

In this study, the primary objective was to examine the various influences of an El Niño event with and without a P-IOD on the PSAC through statistical analysis and numerical simulation. Motivated by the fact that the IOD reaches its peak during boreal autumn and El Niño reaches its peak during boreal autumn to winter, we investigated the influence on the PSAC from boreal autumn to winter during the peak phase for El Niño.

2 DATA, MODEL DESCRIPTION AND EXPERIMENTAL DESIGN

2.1 *Data*

The National Centers for Environmental Prediction/National Center for Atmospheric Research global atmospheric reanalysis data set with 2.5° x 2.5° resolution from January 1960 to December 2010 was the primary data set used in this study. A detailed description of the data assimilation system that produced this data set was given by Kistler et al.[20]. The Hadley Center Sea Ice and SST data set (HadISST1) with a 1° x 1° resolution from January 1960 to December 2010 was also used. Monthly mean data sets were smoothed with a 3-month running average to remove the subseasonal variability (Rayner et al.[21]).

In our study, ENSO and IOD are measured in terms of SST anomalies using the NIÑO3 index and IOD index (IODI), respectively. According to the definition put forward by Saji et al.[9], the IOD index is constructed by the SST anomalous gradient between the WTIO (50°-70°E, 10°S-10°N) and the SETIO (90°-110°E, 10°S-0°). The NIÑO3 index is defined by the SST anomalies averaged over the Niño-3 region (150°-90°W, 5°S-5°N). The P-IOD reaches its peak in boreal autumn, and El Niño reaches its peak from boreal autumn to winter, which shows a seasonal phase locking in the two events. The correlation between the NIÑO3 index and the IODI varied with the evolving seasons, which was significant starting in boreal summer and reached its peak in boreal autumn[8]. In Fig.1, we show the temporal variation in the normalized boreal autumn NIÑO3 index and the IODI from 1960 to 2010.

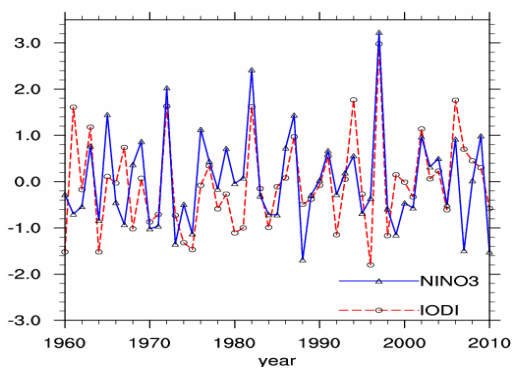

Figure 1. The temporal variation in the normalized boreal autumn NIÑO3 index and IODI from 1960 to 2010

To distinguish the atmospheric circulation characteristics in the SE and EPI years, we first separated the years of El Niño (La Niña) events with and without P-IOD (N-IOD) according to the definition of Rao et al.[22] and Ashok et al.[16] Table 1 displays the above classification with the list of the years.

2.2 *Data*

2.2.1 MODEL DESCRIPTION

The diagnostic results of our study are further verified by the NCAR Community Atmospheric Model 3 (CAM3), which has been widely used in climate studies and served as the atmospheric component of the Community Climate System Model Version 3. A complete description of the CAM3 model can be found in Collins et al.[23]. The model includes two optional ocean models: one drives the atmospheric model by taking the monthly mean SST as a boundary field, called the Data Ocean Model (DOM); the other runs coupled with a simple ocean model. Because the present study focuses on the impact of SSTAs on the atmosphere and rainfall, we adopt the DOM, which drives the model atmosphere by taking the monthly mean SST as a boundary field for our experiments.

Table 1. Years of El Niño (La Niña) events with and without P-IOD (N-IOD).

Type	Year						
Single El Niño	1965	1969	1976	1986	2009		
Single La Niña	1967	1988	1999	2007			
El Niño with P-IOD	1963	1972	1982	1987	1997	2002	2006
La Niña with N-IOD	1964	1971	1975	1984	2005		

2.2.2 EXPERIMENTAL DESIGN

The atmospheric circulation response to El Niño with and without P-IOD is examined by prescribing the composed SSTAs. In the first sensitivity experiments, we impose the SSTAs obtained from averaging the monthly SSTAs of the single El Niño years (1965, 1969, 1976, 1986, 2009) and single La Niña years (1967, 1988, 1999, 2007) over the TP. The experiments are designed to show the influence of a single El Niño and La Niña event and are referred to as SEXP1-P and SEXP1-N, respectively. In the second sensitivity experiments, referred to as SEXP2-P and SEXP2-N, we impose the SSTAs obtained from averaging the monthly SSTAs of El Niño years co-occurring with P-IOD (1963, 1972, 1982, 1987, 1997, 2002, 2006) and La Niña years co-occurring with N-IOD (1964, 1971, 1975, 1984, 2005) over the TP and TIO regions, respectively. The experiments are designed to show the influence of an El Niño (La Niña) event co-occurring with a P-IOD (N-IOD). The SSTAs are imposed from August to the following April. The distribution of SSTAs in September is shown in Fig.2 as an example. The designs of the numerical experiments are given in Table 2.

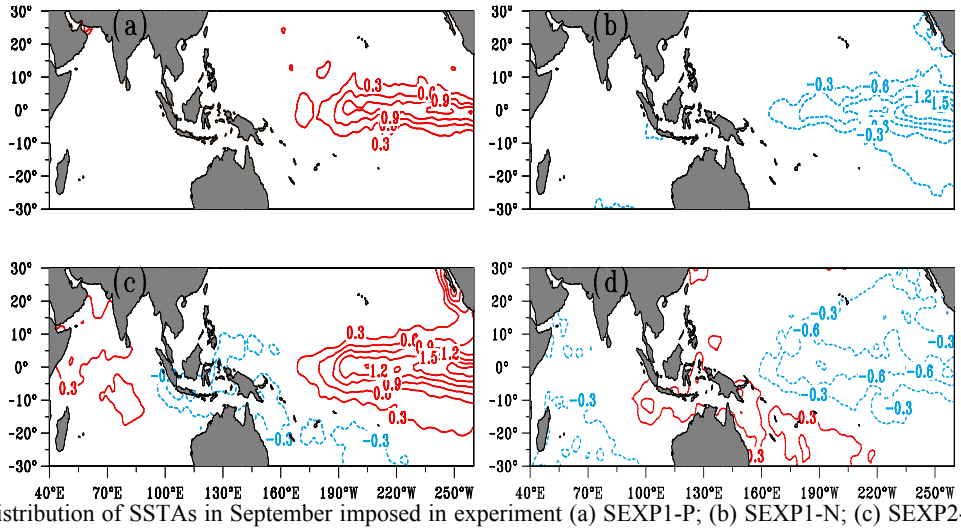

Figure 2. The distribution of SSTAs in September imposed in experiment (a) SEXP1-P; (b) SEXP1-N; (c) SEXP2-P; (d) SEXP2-N (unit: °C).

The last five years of the 20-year integrations of the control run (CTL) are used to construct a 5-member ensemble mean as the model climate to reduce the nonlinear errors caused by different initial conditions. For each of the above sensitivity experiments, the observed composite SSTAs of different events are added to the monthly mean climatological SST field without changing the other parameters. Considering the unforced internal variability, each experiment is started from slightly different initial conditions (for 1 August in the 16th-20th years, which were the last five years in the CTL). The integration runs for nine months (from 1 August to 30 April). The average of five integrations is taken as the result of each sensitivity experiment. Atmospheric circulation anomalies resulting from strong SE and EPI events are obtained by subtracting the results of the SEXP1-P (SEXP2-P) from those of the SEXP1-N (SEXP2-N).

3 ANALYSIS ON SIMULATION RESULTS AND DIFFERENT EVOLUTIONS OF THE PSAC DURING SP AND EPI

In this section, we first examine the relations between the different types of El Niño events and the atmospheric circulation over the NWP using statistical methods. Tending to identify the different impacts between SE and EPI events in the mature phases on atmospheric circulation over the NWP, composited 850 hPa stream function (S_{850}) anomalies of strong SE events (single El Niño minus single La Niña) are shown in Fig.3. In strong SE years, a circulation pattern consists of a north-south pair of elongated

anticyclonic anomalies straddling the Equator over the Maritime Continent. From October to the next January, a complementary pair of anticyclonic anomalies occurs over the southern South China Sea (SCS). The location of S_{850} anomalies during the peak period of SE years is mostly unchanged, with maximum anomalies over the SCS. During the subsequent February the anticyclonic anomalies disappear. The low-level anticyclonic anomaly anchoring near the Philippine Sea during autumn to winter described above was referred to as the PSAC by Wang et al.[24] and Wang and Lin[25] and has been discussed in (Yuan et al.[26]; Yuan and Yang[27]).

Table 2. Designs of the numerical experiment series 1.

Experiment	Application	SST Forcing	Integration
CTL	Obtaining the model climate	The climatological SST varying seasonally within the CAM3	Integration for 20 years from 1 September
SEXP1	Obtaining the single influence of a strong El Niño event	SEXP1-P: SSTA composite from single El Niño years imposed over TP SEXP1-N: SSTA composite from single La Niña years imposed over TP	Integrated from August to the following April
SEXP2	Obtaining the combined influence of a strong El Niño event occurring with P-IOD	SEXP2-P: SSTA (Fig.1 a) composite from strong P-IOD and El Niño events occurring together in a year SEXP2-N: SSTAs (Fig.1 b) composite from strong N-IOD and La Niña events occurring together in a year	Integrated from August to the following April

Composited 850 hPa stream function (S_{850}) anomalies for strong EPI events (El Niño with P-IOD minus La Niña with N-IOD) are displayed in Fig.4. The PSAC showed different evolution features during EPI. During the peak period of EPI, significant anomalous anticyclones on each side of the Equator dominate over the eastern IO and the Maritime Continent in September (Fig.4a). Then, these anticyclones intensify and gradually move eastward from October to November (Fig.4). From December to the subsequent February, the PSAC is located over the Philippine Sea instead of the SCS, which is farther northeastward than in SE years. Furthermore, the PSAC in EPI years can persist until the following spring and summer (figure omitted). Compared to the PSAC during SE, the PSAC during EPI is much stronger (Fig.5), is sustained for a longer time, and occurs farther northeastward. The combined influence of EPI may contribute to this phenomenon.

4 DIFFERENT INFLUENCES OF SE AND EPI EVENTS ON THE PSAC

In this subsection, we present a brief description of anomalous Walker circulation features during SE and EPI. The compositions of anomalous Walker circulation averaged over 5°S and 5°N for strong SE and strong EPI are shown in Fig.6. For SE, significant anomalous rising motions dominate over the tropical eastern Pacific (160°-210°E) from September to the following February, whereas over the equatorial eastern Pacific and the western Indian Ocean, anomalous subsidence motions dominate only from September to October (left panels in Fig.6). For SE, from November to the following February, the anomalous subsidence motions weaken and locate over the tropical western Pacific. Hence, the anomalous sinking motion over the equatorial western Pacific induces dry conditions (Fig.7) and a weak PSAC is produced by the descending Rossby waves associated with the SE-induced subsidence over the Marine Continent and the tropical western Pacific[25].

During EPI, the low-level westerly anomalies over the equatorial Pacific are much stronger than those during SP. Significant anomalous rising motions dominate over the tropical eastern Pacific and the western Indian Ocean, whereas over the equatorial eastern Pacific and the western Indian Ocean, anomalous rising motions dominate from September to November (right panels in Fig.6). Consequently, the anomalous sinking motion over the equatorial western Pacific is much stronger than that during SE and induces much drier conditions, as shown in Fig.7. Due to the strong phase-locking characteristics of the IOD event, which decay in winter, the colder water in the SETIO is weakened and the area is reduced. Therefore, from December to the following February, the rising branch over the equatorial western Indian Ocean is farther east of the SETIO (right panels in Fig.6). Thus, the sinking branch over the equatorial western Pacific is shifted eastward by approximately 10°. The PSAC thus shows different characteristics during EPI, is much stronger, and has a longer lifetime than the PSAC during SP. Furthermore, the

PSAC remains over the SCS from September to November and moves northeastward to the east of the Philippines in the ensuing winter and spring instead of remaining west of the Philippines without change during SE.

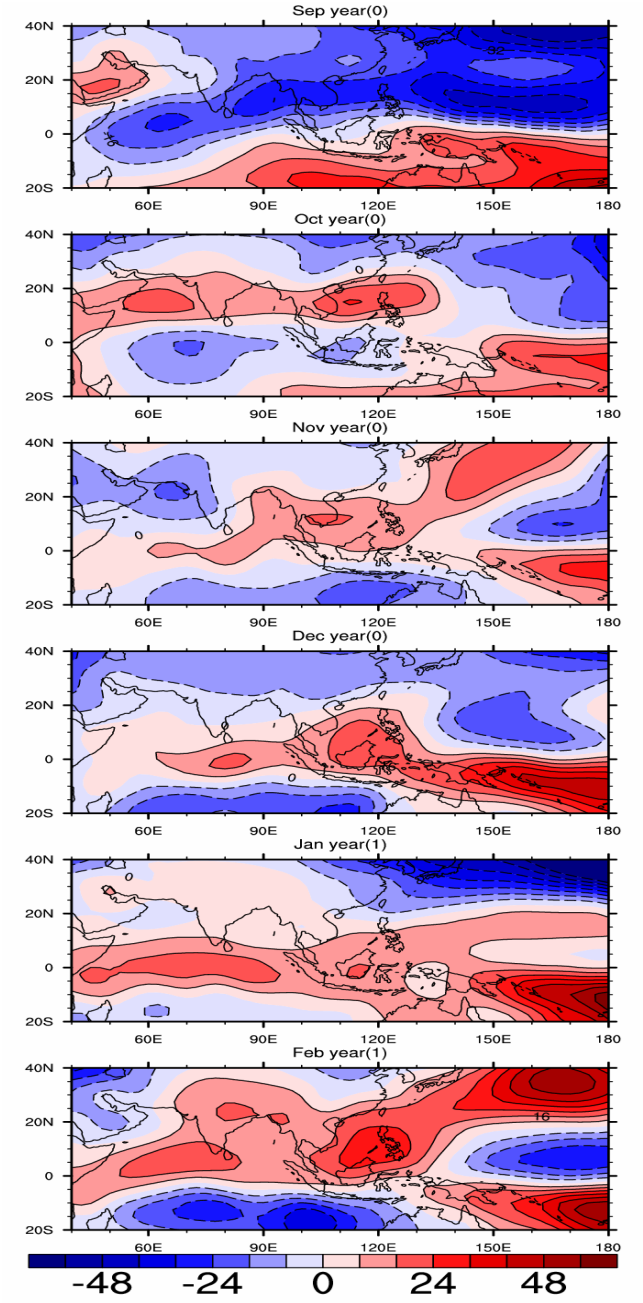

Figure 3. Observational 850 hPa streamfunction anomalies (S_{850}) for strong PE events (single El Niño event years—1965, 1969, 1976, 1986, 2009—minus La Niña event years—1967, 1988, 1999, 2007) from September to the following February (shaded area denotes S_{850} exceeding 8 x 10^5 m^2s^{-1}).

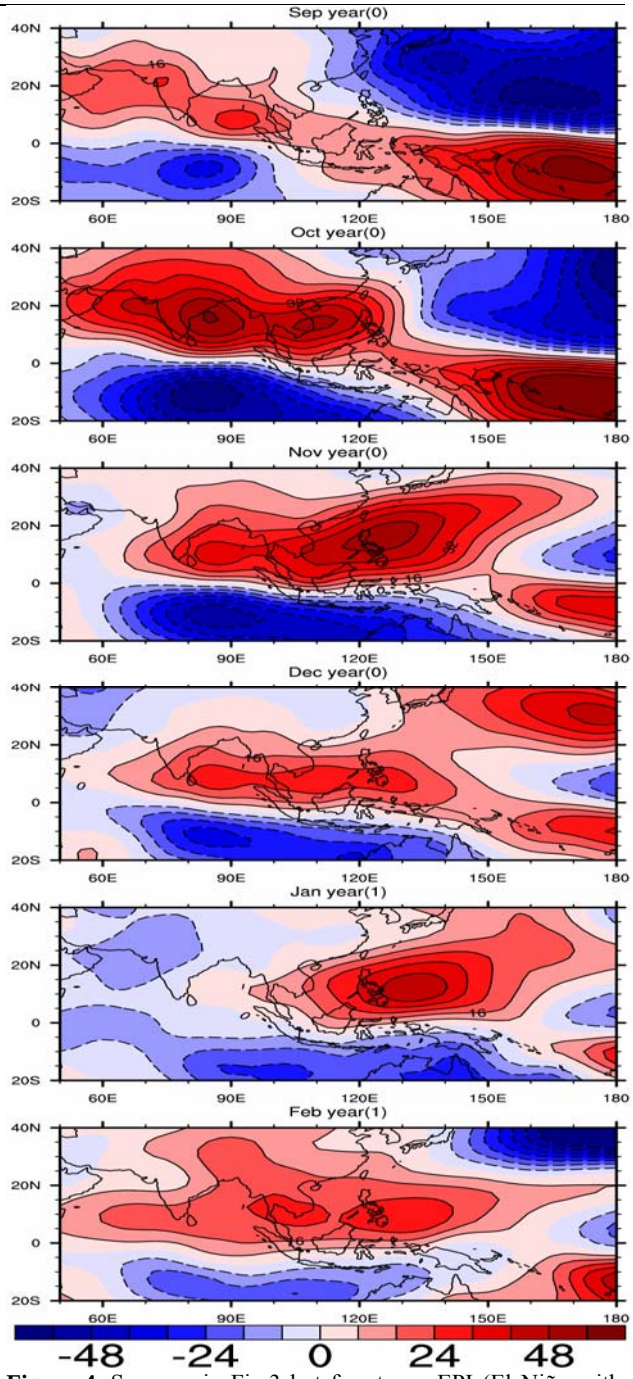

Figure 4. Same as in Fig.3 but for strong EPI (El Niño with P-IOD event years—1963, 1972, 1982, 1987, 1997, 2002, 2006—minus La Niña with N-IOD event years—1964, 1971, 1975, 1984, 1998, 2005).

A more robust method of separating the relative effects of the Pacific and Indian Ocean variability can be achieved using atmospheric model experiments with prescribed SST forcing. Here, sensitivity experiments of SEXP1-PE and SEXP2-PE were conducted to study the impacts of El Niño with and without P-IOD on the PSAC, respectively, using CAM3.0.

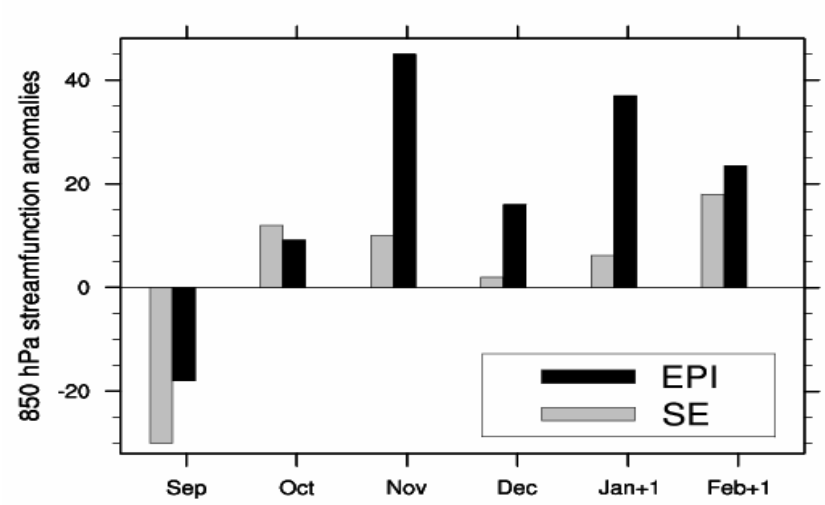

Figure 5. Observational S_{850} anomalies over (120°-150°E, 10°-20°N) of SE and EPI events from September to February of the following year (units: 10^5 m^2s^{-1}).

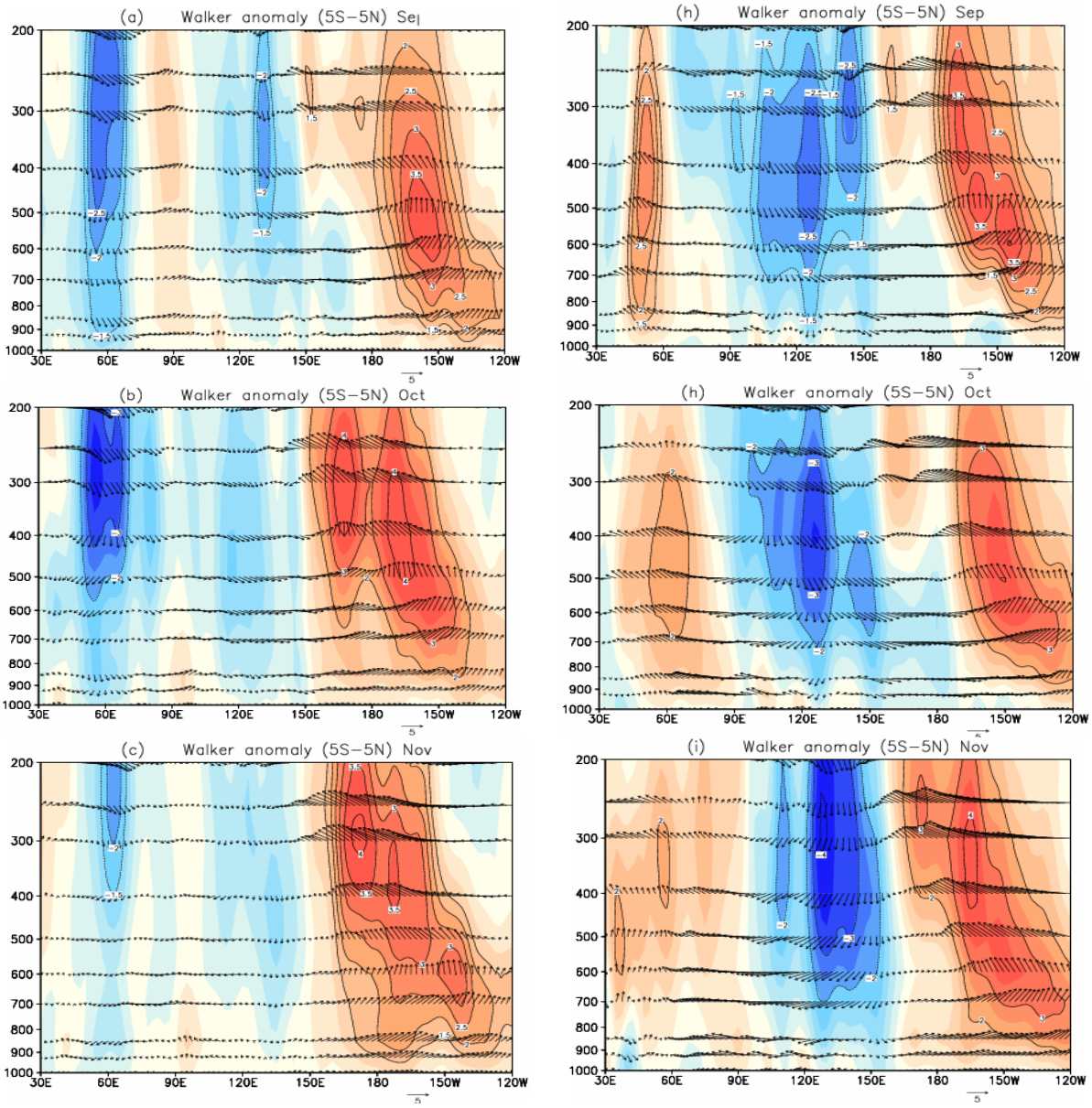

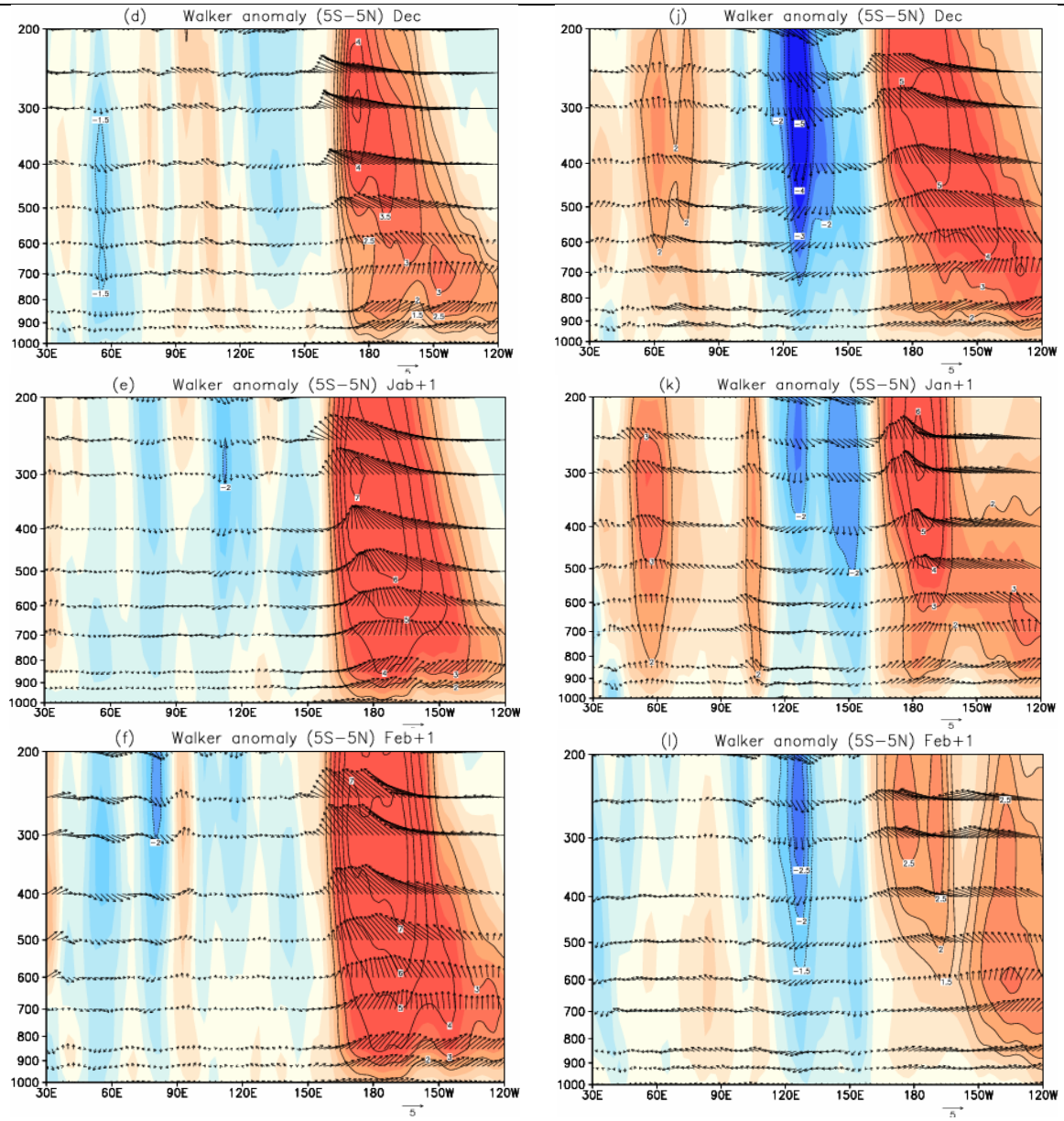

Figure 6. Walker circulation anomalies over 5°S-5°N for single strong El Niño cases (single El Niño event years—1968, 1969, 1989, 2002, 2004—minus La Niña event years—1973, 1975, 1988, 1999) during the developing and mature phases, from Fig.5a to Fig.5f; strong co-occurring events (El Niño with P-IOD event years—1963, 1972, 1982, 1987, 1997—minus La Niña with N-IOD event years—1964,1971,1975, 1984,1988), from Fig.5g to Fig.5l.

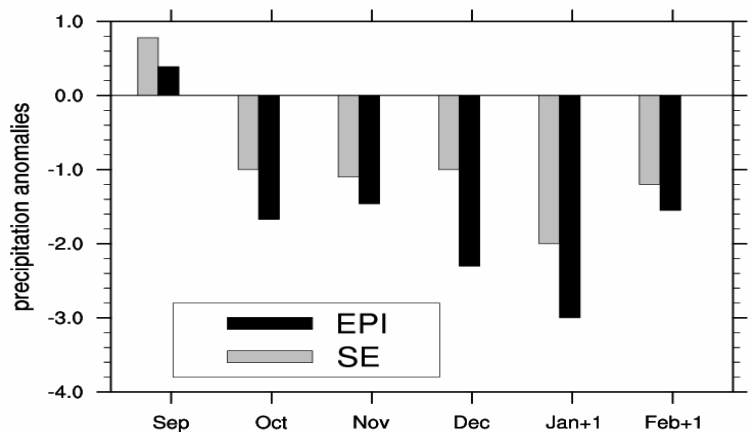

Figure 7. Observational month precipitation anomalies over 120°-140°E, 0°-15°N for strong SE and strong EPI from September to the following February (units: mm day^{-1}).

Wind anomalies of 850 hPa are produced over the tropical ocean resulting from the effects of El Niño with and without P-IOD (Figs.8 and 9). In Fig.8, from September to the following February, significant westerly anomalies occur over the central TP and almost no noticeable wind anomalies occur over the TIO. This pattern suggests that during the mature phase of SE, the changes in the SST pattern over the TP cause a change in the seasonal westerly surface winds along the Equator. The anomalous Walker circulation appears to be the reverse of the normal condition; the convection in the west is suppressed, whereas the convection in the eastern TP is strengthened. Because the convection is suppressed in the western TP, SE causes dry conditions over Indonesia (Fig.10). Furthermore, during an SE year, no meaningful anticyclone circulation anomaly can be observed over the Philippine Sea until December, which then persists until January of the following year (Fig.8).

In the EPI years, from September to the following February, strong surface divergent westerly anomalies occur over the central TP and easterly anomalies occur over the TIO (Fig.9). Such strong surface easterlies over the TIO cannot be found in the above-mentioned SE years in Fig.8. This pattern indicates that changes have occurred in the Indo-Pacific Walker circulation. Thus, we calculate the 500 hPa vertical velocity anomaly difference between the equatorial eastern Pacific (5°S-5°N, 160°-120°W) and the equatorial western Pacific (5°S-5°N, 120°-160°E) as an index of the Walker circulation (Wang et al.[28]). The results show that in EPI years, the anomalous Walker circulation is much stronger than in SE years. It can also be demonstrated that in co-occurring years, the effect of P-IOD can enhance the Walker circulation anomalies in the Indo-Pacific region, resulting in a much drier precipitation condition over the western TP (Fig.11). Furthermore, during the autumn of an EPI year, the PSAC is established over the southern SCS. The PSAC moves to the Philippines in December, intensifies and moves northeast of the Philippines in January of the following year (Fig.9), and persists into the following spring and summer (figure omitted). All of the simulation results roughly coincide with the observations.

The simulations and statistical analyses strongly indicate that El Niño with P-IOD tends to produce a stronger suppressing movement in the Indo-Pacific region and results in a stronger PSAC there.

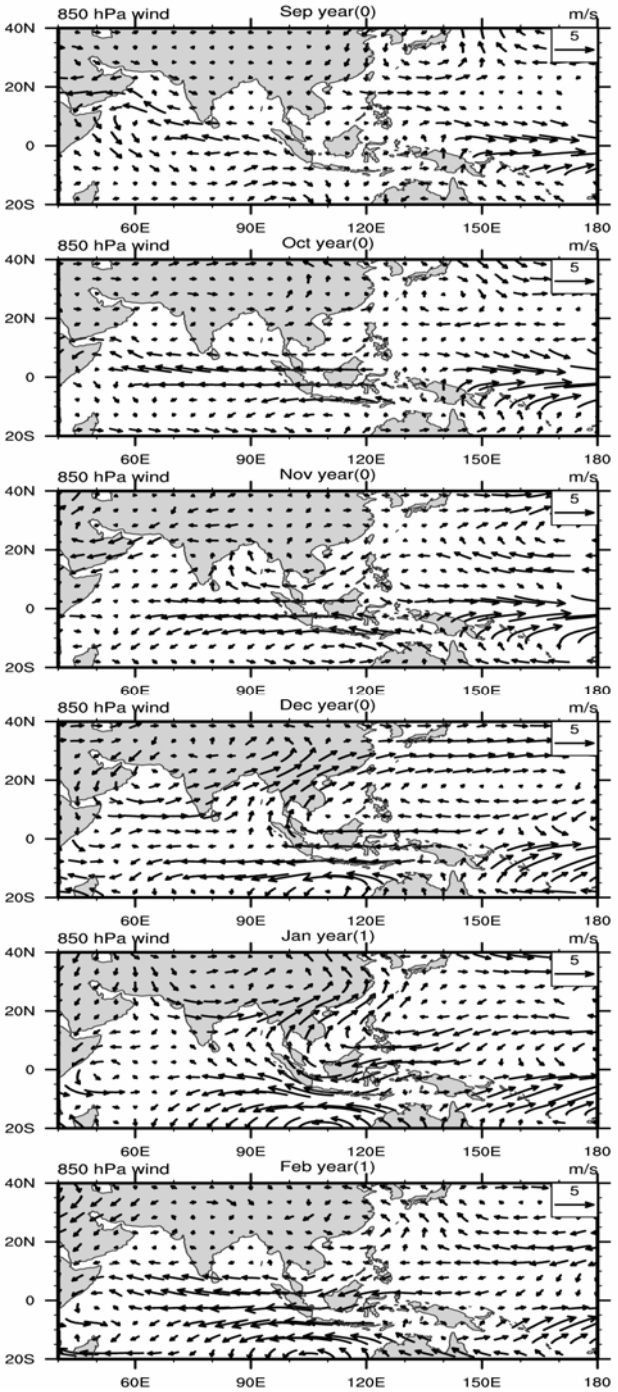

Figure 8. The simulated 850 hPa wind anomalies during a strong SE (El Niño minus La Niña) from September to the following February (units: ms^{-1}).

5 SUMMARY AND DISCUSSION

This paper examines the influences of El Niño with and without P-IOD in the preceding autumn on atmospheric circulation over the NWP. A composite analysis was carried out in this study. Additionally, we conducted several multi-ensemble sensitivity experiments using CAM3 with various types of SST fields as a lower boundary forcing to assess the

influence of SE and EPI. The results strongly show that the PSAC excited by SE tends to be weaker and has a shorter lifetime than that excited by EPI. This finding indicates that a P-IOD may be an important factor to consider to improve the predictability of the East Asian climate during ENSO, which can amplify the PSAC when El Niño exerts it. In other words, an EPI tends to produce a stronger PSAC and less precipitation over the NWP than an SE does.

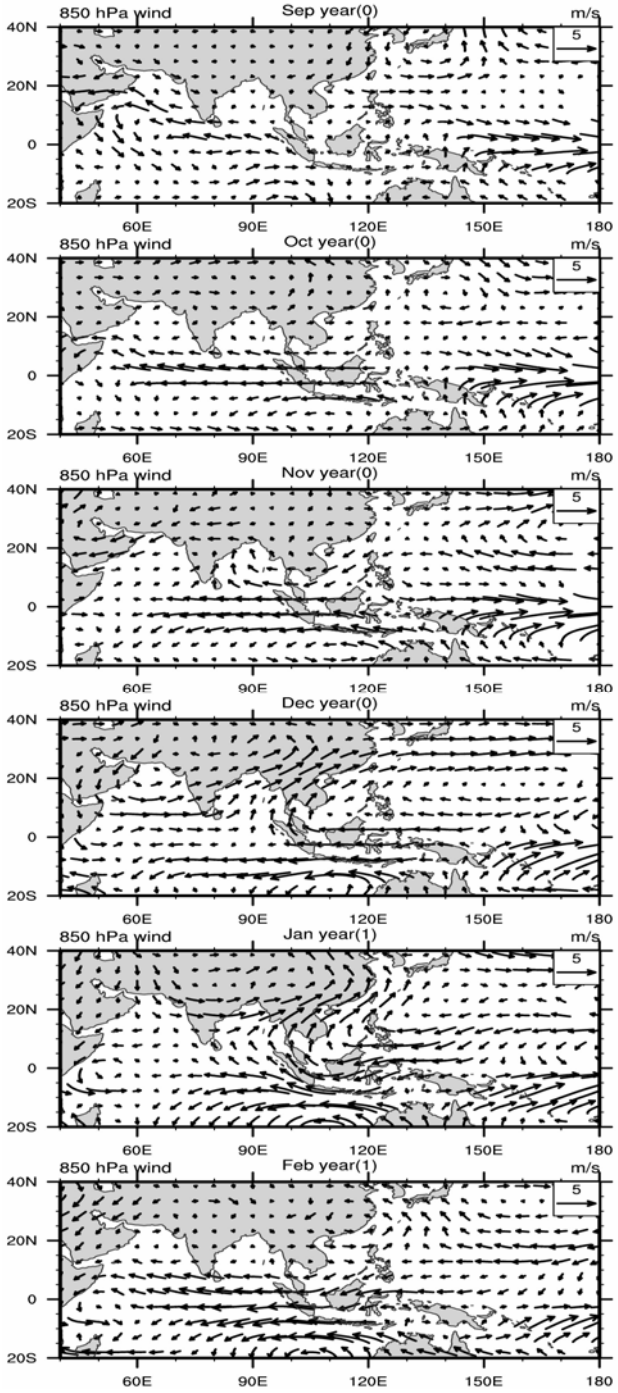

Figure 9. As in Fig.8 except for a strong EPI (El Niño with P-IOD minus La Niña with N-IOD).

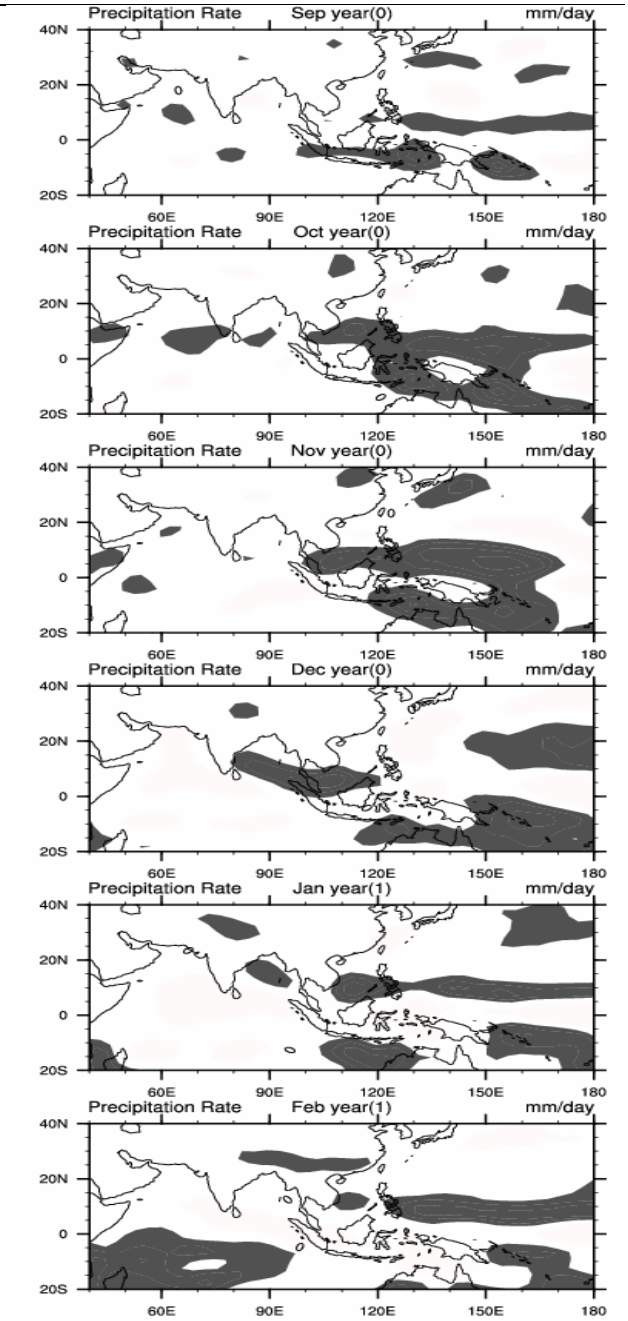

Figure 10. The simulated precipitation anomalies for a strong SE (El Niño minus La Niña) during the developing and mature phases (negative precipitation areas ≤ -1 mm day^{-1} are shaded; units: 1 mm day^{-1}).

When a P-IOD event simultaneously occurs with El Niño in the mature phase, the influence on the atmospheric circulation over the NWP is amplified through a greater development of the PSAC. The significant negative SSTAs over the SETIO and the western TP, when both events mature in autumn, can induce a negative anomalous Walker circulation in the TP and form an anomalous Walker cell over the TIO regions separate from the Walker cell over the TP (Fig.6), although the intensity of the SSTAs over TIO and TP can gradually decrease with time. Thus, the low-level divergence center over the TWP that

occurred during EPI is much strengthened. The sinking branch over the TWP-Maritime Continent is substantially intensified in this case, which appears as part of an anti-Walker circulation.

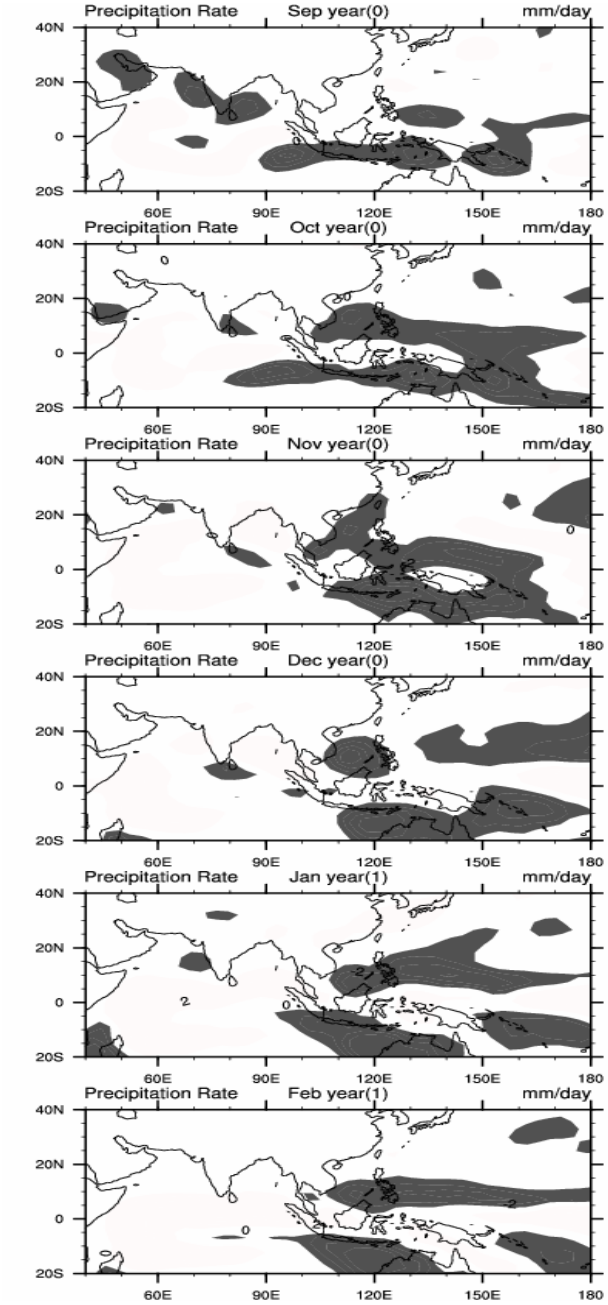

Figure 11. Simulated precipitation anomalies for a strong EPI (El Niño with P-IOD minus La Niña with N-IOD). Negative precipitation areas ≤ -1 mm day^{-1} are shaded; units: 1 mm day^{-1}.

The anomalous sinking over the TWP-Maritime Continent also appears in SE (Fig.6), but the intensity is weaker and the location remains unchanged instead of being pushed farther northeastward. Thus, the convection under the influence of EPI is suppressed to a greater degree and causes much drier conditions over the TWP-Maritime Continent than does a single event. Correspondingly, a stronger anomalous sinking motion dominates over the eastern IO and tropical western Pacific, exciting two anomalous low-level anticyclones located symmetrically to both sides of the Equator through the Rossby wave response. The northern anticyclone is suggested to arise due to the development of the PSAC during EPI, which is much stronger and has a longer lifetime. As a result, the stronger PSAC can persist from boreal fall to the ensuing summer (figure omitted). Consistent with the observation results, the simulations also suggest that the P-IOD event can weaken the Indian Ocean-Walker circulation, and when P-IOD occurs with El Niño, the anomalous subsidence over the TWP-Maritime Continent is enhanced. This study suggests that a positive IOD event tends to exert a prominent influence on the PSAC during an El Niño event and that there is a combined impact of the El Niño with P-IOD on the development of the PSAC. It is important to consider the coupled atmosphere-ocean interaction over the TIO to improve our understanding and prediction accuracy regarding the East Asian climate during ENSO.

REFERENCES:

[1] YAN Hong-ming, LI Qing-quan, YUAN Yuan, et al. Circulation variation over western North Pacific and its association with tropical SSTA over Indian Ocean and the Pacific [J]. Chin J Geophs, 2013, 58(8): 2 542-2 557 (in Chinese).

[2] CHUNG P H, SUI C H, LI T M. Interannual relationships between the tropical sea surface temperature and summertime subtropical anticyclone over the western North Pacific [J]. J Geophys Res, 2011,116, D13111, doi:10.1029/2010 JD015554

[3] CHOU C. Establishment of the low-level wind anomalies over the Western North Pacific during ENSO development [J]. J Climate, 2004, 17(6): 2 195-2 212.

[4] WANG B, WU R, FU X H. Pacific-the East Asian teleconnection: How does ENSO affect the East Asian climate? [J]. J Climate, 2000, 13(9): 1 517-1 536.

[5] WANG Y F, WANG B, OH Jai-Ho. Impact of Preceding El Niño on the East Asian Summer Atmosphere Circulation[J]. J Meteorol Soc, 2001, Japan, 79(1B): 575-588.

[6] WU B, LI T, ZHOU T. Relative contributions of the Indian Ocean and local SST anomalies to the maintenance of the western North Pacific anomalous anticyclone during the El Niño decaying summer [J]. J Climate, 2010, 23: 2 974-2 980.

[7] HE Chao, ZHOU Tian-jun, ZOU Li-wei, et al. Two interannual variability modes of the Northwestern Pacific Subtropical Anticyclone in boreal summer [J]. Sci China: Earth Sci, 2012, 42 (12): 1 923-1 936 (in Chinese).

[8] LI Y, WANG Y F, MU Lin et al. Impact of preceding El Niño and the Indian Ocean Dipole on the southern China precipitation in early summer [J]. Adv Meteorol, 2014, http://dx.doi.org/10.1155/2014/450691.

[9] SAJI N H, GOSWAMI B N, VINAYACHANDRAM P N, et al. A dipole mode in the tropical Indian Ocean [J]. Nature, 1999, 401: 360-363.

[10] WEBSTER P J, MOORE A M, LOSCHNING J P, et al. Coupled ocean- atmosphere dynamics in the Indian Ocean

during 1997-98 [J]. Nature, 1999, 401: 356-360.
[11] LUO J J, MASSON S, BEHERA S, et al. Experimental forecasts of the Indian Ocean dipole using a coupled OAGCM [J]. J Climate, 2007, 20: 2 178-2 190.
[12] XIANG B, YU W, LI T, et al. The critical role of the boreal summer mean state in the development of the IOD [J]. Geophys Res Lett, 2011, 38, L02710, doi:10.1029/2010GL045851.
[13] MEYER G, MCINTOSH P, PIGOT L, et al. The years of El Niño, La Niña, and interactions with the tropical Indian Ocean [J]. J Climate, 2007, 20: 2 872-2 880.
[14] SAJI N H, YAMAGATA Y. Structure of SST and surface wind variability during Indian Ocean Dipole Mode events: COADS observations [J]. J Climate, 2003, 16(16): 2 735-2 751.
[15] ASHOK K, GUAN Z, YAMAGATA T. Impact of the Indian Ocean Dipole on the Decadal Relationship between the Indian Monsoon Precipitation and ENSO [J]. Geophys Res Lett, 2001, 28(23): 4 499-4 502.
[16] ASHOK K, GUAN Z, SAJI N H, YAMAGATA T. Individual and combined influences of ENSO and Indian Ocean Dipole on the Indian summer monsoon [J]. J Climate, 2004, 17(16): 3 141-3 155.
[17] GUAN Z Y, YAMAGATA T. The unusual summer of 1994 in East Asia: IOD Teleconnections [J]. J Geophys Res Lett, 2003, 30(10): 1 544-1 548.
[18] HONG C C, LU M M, KANAMITSU M. Temporal and spatial characteristics of positive and negative Indian Ocean dipole with and without ENSO [J]. J Geophys Res Lett, 2008, 113, D08107, doi:1029/ 2007J D009151.
[19] CHERCHI A, NAVARRA A. Influence of ENSO and of the Indian Ocean Dipole on the Indian summer monsoon variability [J]. Climate Dyn, 2013, 41(1): 81-103.
[20] KISTLER R, Coauthors. The NCEP-NCAR 50 year reanalysis: Monthly means CD-ROM and documentation [J]. Bull Amer Meteorol Soc, 2001, 82(2): 247-268.
[21] RAYNER N A., PARKER D E, HORTON E B, et al. Global analyses of sea surface temperature, sea ice, and night marine air temperature since the late nineteenth century [J]. J Geophys Res, 2003, 108,4407,doi:10.1029/2002JD002670.
[22] RAO A S, BEHERA S K, MASUMOTO Y, et al. Interannual subsurface variability in the tropical Indian Ocean with special emphasis on the Indian Ocean dipole [J]. Deep-sea Res, 48B, 1 549-1 572.
[23] COLLINS W D, RASCH P J, BOVILL B A, et al. Description of the NCAR Community Atmosphere Model (CAM3.0) [M]. Boulder: National Center for Atmospheric Research, 2004, NCAR/TN-464+STR, 1-226.
[24] WANG B, WU R G, FU X H. Pacific-East Asian teleconnection: how does ENSO affect East Asian climate? [J] J Climate, 2000, 13(9): 1 517-1 536.
[25]WANG B and LIN H. Rainy season of the Asian-Pacific summer monsoon [J]. J Climate, 2002, 15: 386-398.
[26] YUAN Y, YANG S, ZHANG Z Q. Different Evolutions of the Philippine Sea Anticyclone between the Eastern and Central Pacific El Niño: Possible Effects of Indian Ocean SST [J]. J Climate, 2012, 25(22): 7 867-7 883.
[27] YUAN Y, YANG S. Impact of Different Types of El Niño on the East Asian Climate Focus on ENSO Cycles [J]. J Climate, 2012, 25(21): 7 702-7 722.
[28] WANG C, WANG X, FLORIDA M, et al. Classifying El Niño Modoki I and II by Different Impacts on Rainfall in Southern China and Typhoon Track [J]. J Climate, 2013, 26(4): 1 322-1 338.

Citation: LI Yan, WANG Qing-yuan, MU Lin, et al. Different evolutions of the Philippine Sea anticyclone for the impact of El Niño in peak phases with and without a positive Indian Ocean Dipole [J]. J Trop Meteorol, 2015, 21(S1): 23-33.